

Supplemental Data

Hair Follicle Stem Cells Are Specified

and Function in Early Skin Morphogenesis

Jonathan A. Nowak, Lisa Polak, H. Amalia Pasolli, and Elaine Fuchs

Supplemental Experimental Procedures

Histology

Primary antibodies and dilutions used were: AE13 and AE15 (mouse, 1:50 and 1:20, T.T. Sun, New York University, New York), Blimp1 (mouse, 1:100, R. Tooze, University of Leeds, Leeds), BrdU (rat, 1:200, Abcam), active Caspase-3 (rabbit, 1:1000, R & D), CD34 (rat, 1:100, BD-Pharmingen), Cdk4 (rabbit, 1:200, Santa Cruz), E- and P-Cadherin (rat, 1:100, M. Takeichi, RIKEN, Kobe), Gata-3 (mouse, 1:100, Santa Cruz), α 6- and β 4-Integrin (rat, 1:200, BD-Pharmingen), Involucrin (rabbit, 1:1000, Covance), K5 (rabbit, 1:2000, Fuchs Lab), K14 (rabbit, 1:500, Fuchs Lab), K1 (rabbit, 1:250, Fuchs Lab), K6 (rabbit, 1:500, Fuchs Lab), K17 (rabbit, 1:4000, P. Coulombe, Johns Hopkins, Baltimore), Ki67 (rabbit, 1:500, NovoCastra), Lef1 (rabbit, 1:250, Fuchs Lab), Lhx2 (rabbit, 1:2000, T. Jessell, Columbia, New York), Loricrin (rabbit, 1:300, Fuchs Lab), Nfatc1 (mouse, 1:100, Santa Cruz), p63 (rabbit, 1:200, Santa Cruz), PPAR γ (rabbit, 1:200, Santa Cruz), Sox9 (rabbit, 1:200, Santa Cruz), and Tcf3 (guinea pig, 1:200, Fuchs Lab). Secondary antibodies coupled to FITC or Rhodamine Red-X were from Jackson Laboratories. Imaging was performed using Zeiss Axioskop and Axiophot microscopes equipped with Spot RT (Diagnostic Instruments) and Axiocam (Zeiss) digital cameras, respectively. In several cases, composite immunofluorescence images of HF and skin (labeled Low Mag) were created by manually aligning overlapping images of adjacent skin sections.

HF length was quantified using MetaMorph software by measuring the linear distance along an in-plane follicle from the bottom of the leading edge/matrix to the epidermis. A minimum of 100 HF from each genotype were analyzed for each time point. Developmental staging was performed

according to standard classification (Schmidt-Ullrich and Paus, 2005) on 10 10x fields from 3 WT and 3 cKO mice. Quantification of proliferation in the upper ORS for BrdU pulse incorporation and Ki67 expression experiments was performed by analyzing the uppermost 20 cells on both sides of the K5/E-Cadherin positive ORS for each follicle. Matrix size was measured by counting the number of Ki67 positive cells at the base of 20 HFs for WT and cKO at each time point. BrdU pulse-chase analysis of matrix proliferation and differentiation kinetics was performed on 10 HFs from WT and cKO mice at each time point in three separate labeling experiments. Hair keratin expression detected by AE13 indicated the zone of differentiating cells, while ORS cells were recognized by their location at the edge of the follicle and unique elongated nuclear shape.

Electron Microscopy

For scanning EM, samples were fixed in 2% glutaraldehyde, 4% PFA, and 2 mM CaCl₂ in 0.05 M sodium cacodylate buffer, pH 7.2, at RT for >1 h, dehydrated, critical-point dried, mounted, and sputter coated with gold-palladium. For transmission EM, samples were fixed as described for scanning EM, postfixed in 1% osmium tetroxide, and processed for Epon embedding; ultrathin sections (60–70 nm) were counterstained with uranyl acetate and lead citrate.

Scanning EM images were obtained using a field emission scanning electron microscope (model 1550; LEO Electron Microscopy, Inc.), and transmission EM images were taken with a transmission electron microscope (Tecnai G2-12; FEI) equipped with a digital camera (model XR60; Advanced Microscopy Techniques, Corp.)

Supplemental Figures

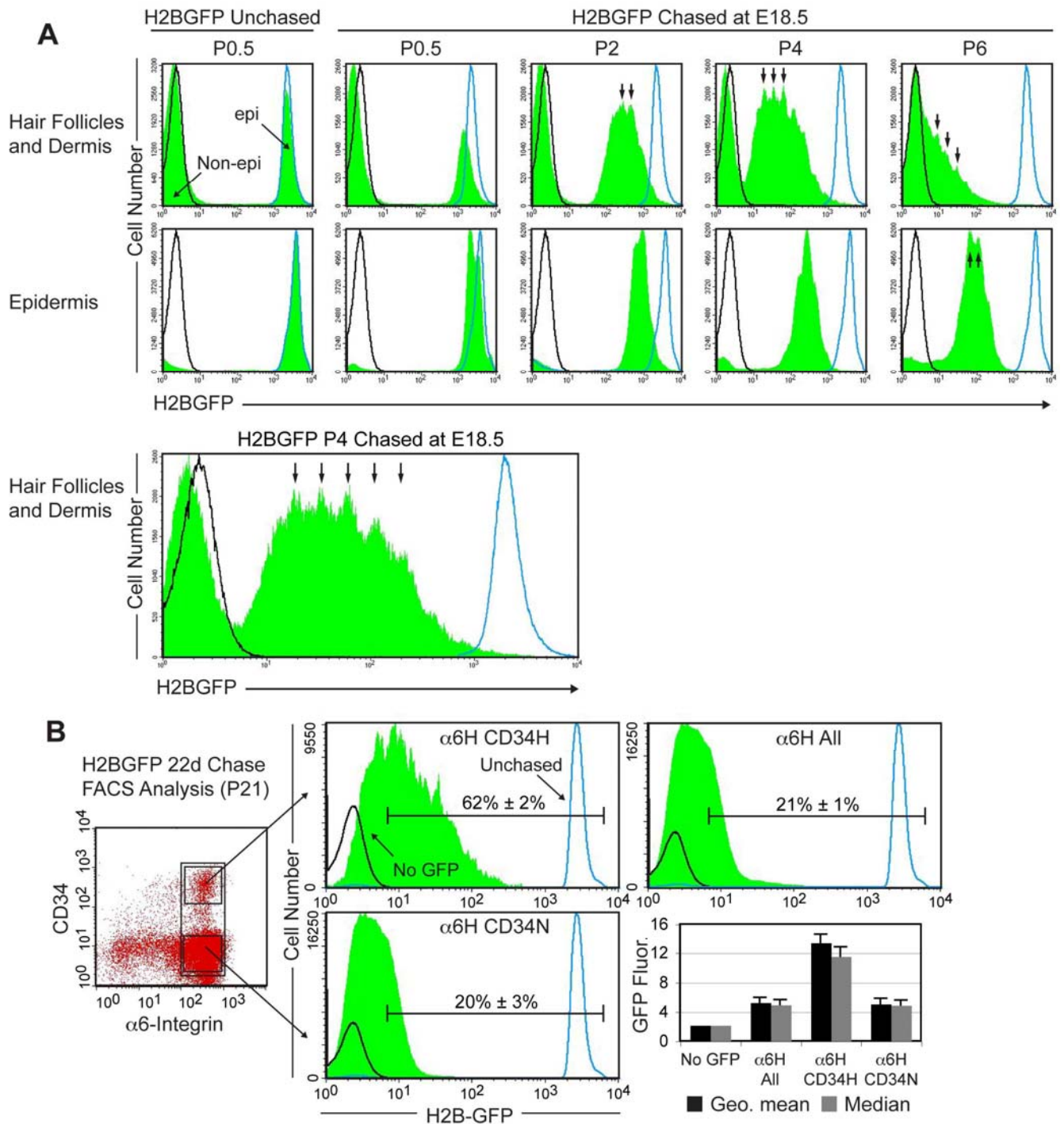


Figure S1. FACS Analysis of Chased H2BGFP Mice Reveals the Early Appearance of a LRC Population. (A) FACS analysis of HF/dermis and epidermis from P0.5-P6 mice. Within each population, GFP intensity is represented as a green histogram, with overlays from non-GFP mice (black) and unchased *H2BGFP* mice (blue) representing minimum and all maximum endpoints for

detecting H2BGFP fluorescence. Label dilution is detectable 24 hours after the beginning of the chase period (compare chased and unchased P0.5 mice). Within the GFP spectrum, peaks (denoted by arrows) were often spaced at 2-fold intervals, consistent with cells losing 50% of their H2BGFP label at each division. Note that the pattern of HF label retention is asymmetric compared to label retention in the epidermis, and that a tail of LRCs is detectable in P4 and P6 HF histograms. The existence of GFP negative cells (Non-epi) in all HF plots, including unchased mice, is reflective of the non-epithelial cells types (dermal papilla, dermal fibroblasts, melanocytes) that co-purify during HF isolation. **(B)** FACS analysis of skin epithelial cells isolated from P21 mice chased beginning at E18.5. Black boxes on dot plot indicate gates for bulge SCs (α 6HCD34H), non-bulge basal cells (α 6HCD34N) and all basal cells (α 6H) (H, high; N, negative). Horizontal bars indicated percentage of cells (\pm SD) with detectable fluorescence. Note that the α 6HCD34H histogram spans a wider range of fluorescent intensity than α 6HCD34N and α 6H histograms and contains more H2BGFP-positive cells. Graph displays quantification of GFP fluorescence levels in all three populations. GFP negative mice are shown as a control. Note higher geometric mean and median fluorescence levels in the α 6HCD34H population. Errors bars represent one standard deviation.

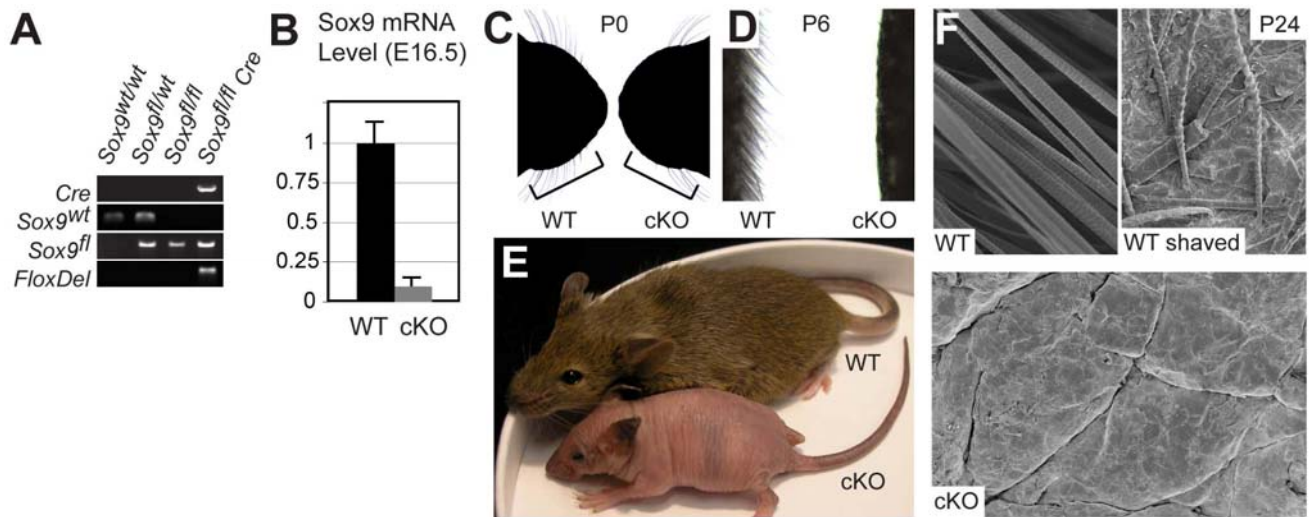


Figure S2. Embryonic Ablation of Sox9 in the Skin by *K14-Cre* Results in the Failure to Form a Hair Coat. (A) Representative genotyping results from E16.5 skin show specific detection of *Sox9^{WT}*, *Sox9^{Flox}*, and *Sox9^{FloxDel}* alleles and demonstrate deletion of floxed *Sox9* alleles by *K14-Cre*. (B) RT-PCR analysis of *Sox9* mRNA levels in E16.5 epidermis shows a greater than 10-fold decrease in *Sox9* expression in cKO compared to WT. Error bars represent one standard deviation. (C) *Sox9* cKO P0 mice display an 80% reduction in whisker number compared to WT mice. (D) Analysis of P6 backskin shows *Sox9* cKO mice fail to form a visible pelage hair coat. (E) Gross appearance of adult WT and cKO mice showing profound lack of hair on cKO. Adult cKO mice were consistently smaller than WT mice, and the abundant expression of *Sox9* in the K14-positive epithelial portion of salivary glands suggests that impaired feeding is a possible cause of smaller size. (F) Scanning electron microscopy of adult backskin demonstrates a total absence of hair on cKO backskin. Shaving the hair coat of WT mice reveals the surface of the epidermis and the insertion points of hair shafts.

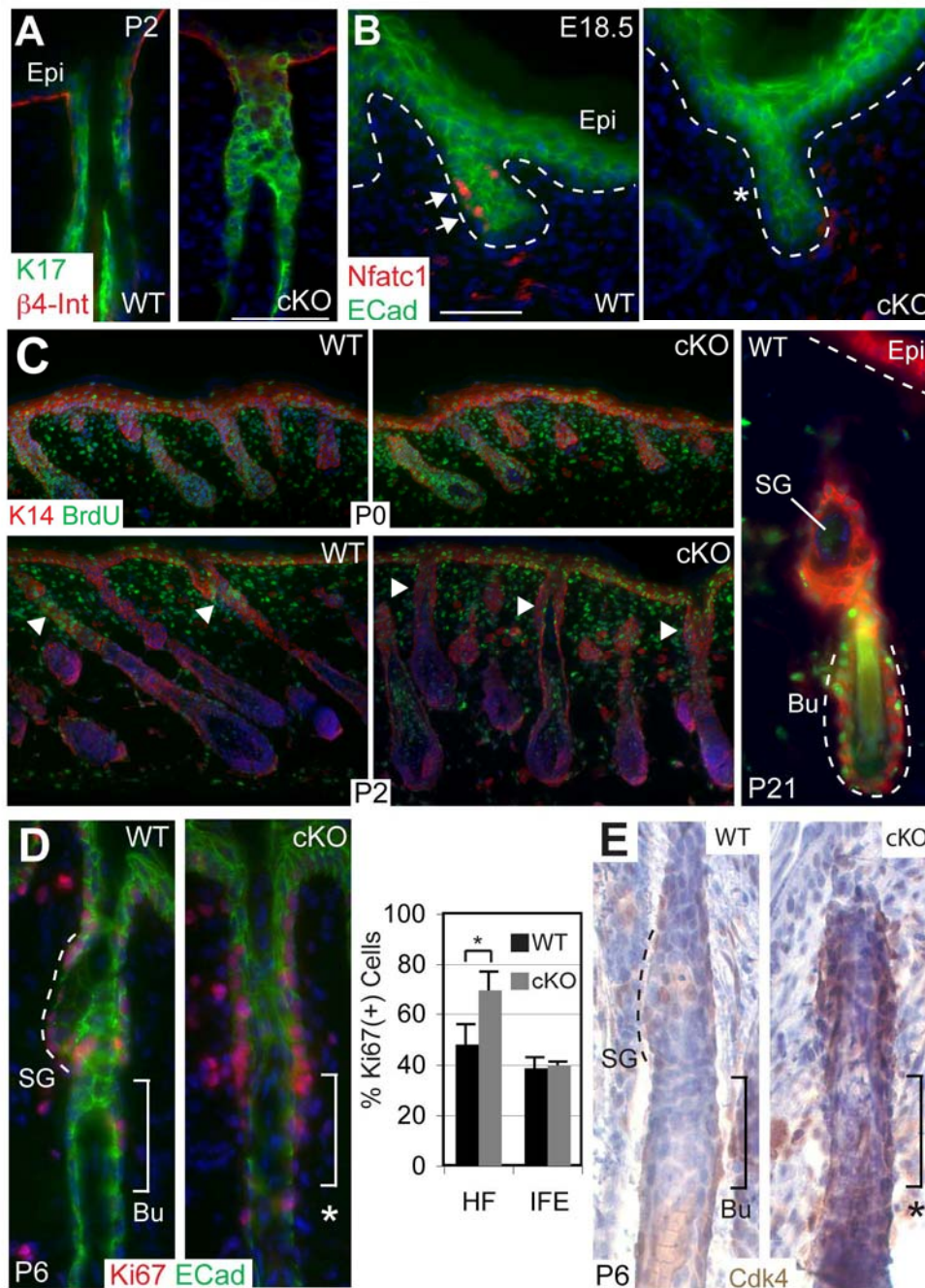


Figure S3. Maintenance of General ORS character, but Loss of Quiescence in the Presumptive Bulge Region of Sox9 cKO HF Indicates a Specific Absence of Early SCs. (A) Immunofluorescence microscopy shows that general ORS marker keratin 17 (K17) remains properly expressed in cKO HF. β 4-Int, β 4-Integrin. **(B)** Nfatc1, marking developing early bulge cells (arrows) is absent at E18.5 in cKO HF (asterisk). Dotted lines indicate epidermal-dermal border. ECad, E-Cadherin. **(C)** A 24h BrdU pulse was administered to mice at E17.5-E18.5. Immunofluorescence

microscopy on P0 skin indicates complete BrdU labeling of all cells in the keratin 14 (K14) positive epidermis and HF of WT and cKO mice. As early as P2, clusters of BrdU positive LRCs (arrowheads) begin to appear in the upper portions of WT follicles, but are less apparent in cKO follicles. Examination of LRCs in WT P21 HF reveals exclusive localization in the adult bulge niche (Bu). **(D)** Immunofluorescence microscopy for Ki67 expression shows an increase in average percentage of Ki67 positive proliferating cells in the upper ORS of cKO HF (69%) compared to WT (48%). Note the marked increase in Ki67 positive cells in the cKO approximate bulge area (bracket, asterisk) compared to WT (bracket, Bu). Proliferation rates in the interfollicular epidermis, as measured by Ki67 expression, are identical in WT and cKO skin. Graph shows average data (\pm SEM) from three separate WT and cKO mice. **(E)** Immunohistochemistry shows an increase in Cdk4 expression in the entire ORS of cKO mice compared to WT, indicative of enhanced proliferation. SG, sebaceous gland.

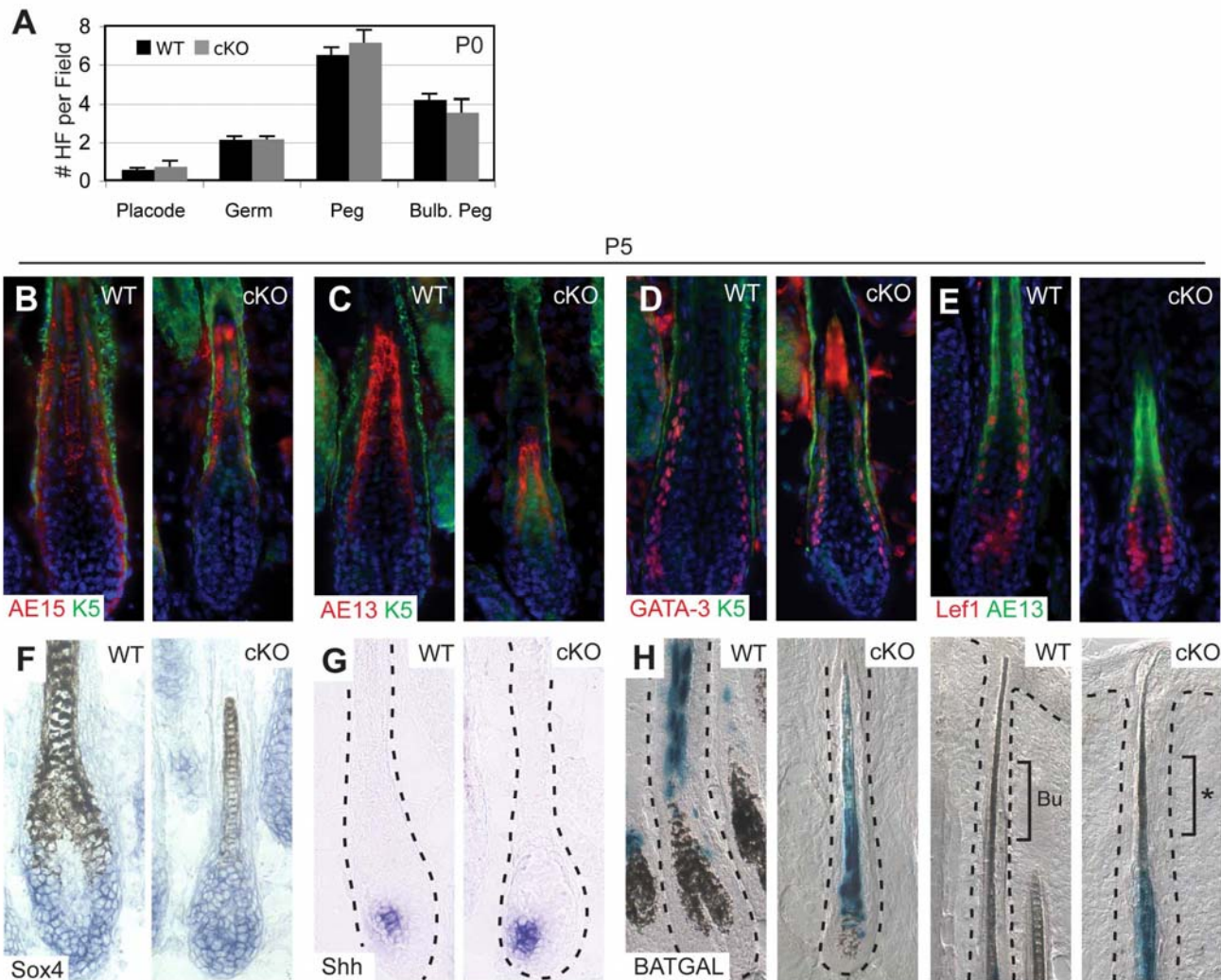


Figure S4. Hair Follicle Specification and the Program of Hair Differentiation are Unimpaired in Sox9 cKO Skin Lacking Early SCs. (A) Analysis of P0 backskin reveals that the absence of Sox9 does not affect follicle number or developmental stage. Error bars represent SEM. (B-E) Immunofluorescence microscopy on P5 HF cross-sections demonstrates that structural proteins such as trichohyalin (AE15), an inner root sheath (IRS) marker, and hair keratin (AE13), a hair shaft marker of the cortex and medulla, were correctly expressed in the appropriate subbasal layers of Sox9-deficient HF cross-sections. Transcription factors such as GATA-3 and Lef1, which are key regulators of differentiating IRS and pre-cortical cells, respectively, were also expressed correctly. (F-G) In situ hybridization demonstrates no abnormalities in Sox4 or Shh expression, which in anagen-phase postnatal HF cross-sections, precede GATA-3 and Lef1, but are downstream of Sox9. Black dotted lines indicate the dermis/HF border. (H) Xgal staining on skin sections obtained by breeding to the Wnt reporter

mouse *BATGAL* revealed that Sox9-deficiency did not appear to perturb Wnt signaling within the precursor cells that generate the hair shaft of cKO follicles (Figure S5H). Notably, although Sox9 has been implicated as a repressor of Wnt/ β -catenin signaling (Akiyama et al., 2004), *BATGAL* expression did not appear to be activated in the cKO ORS.

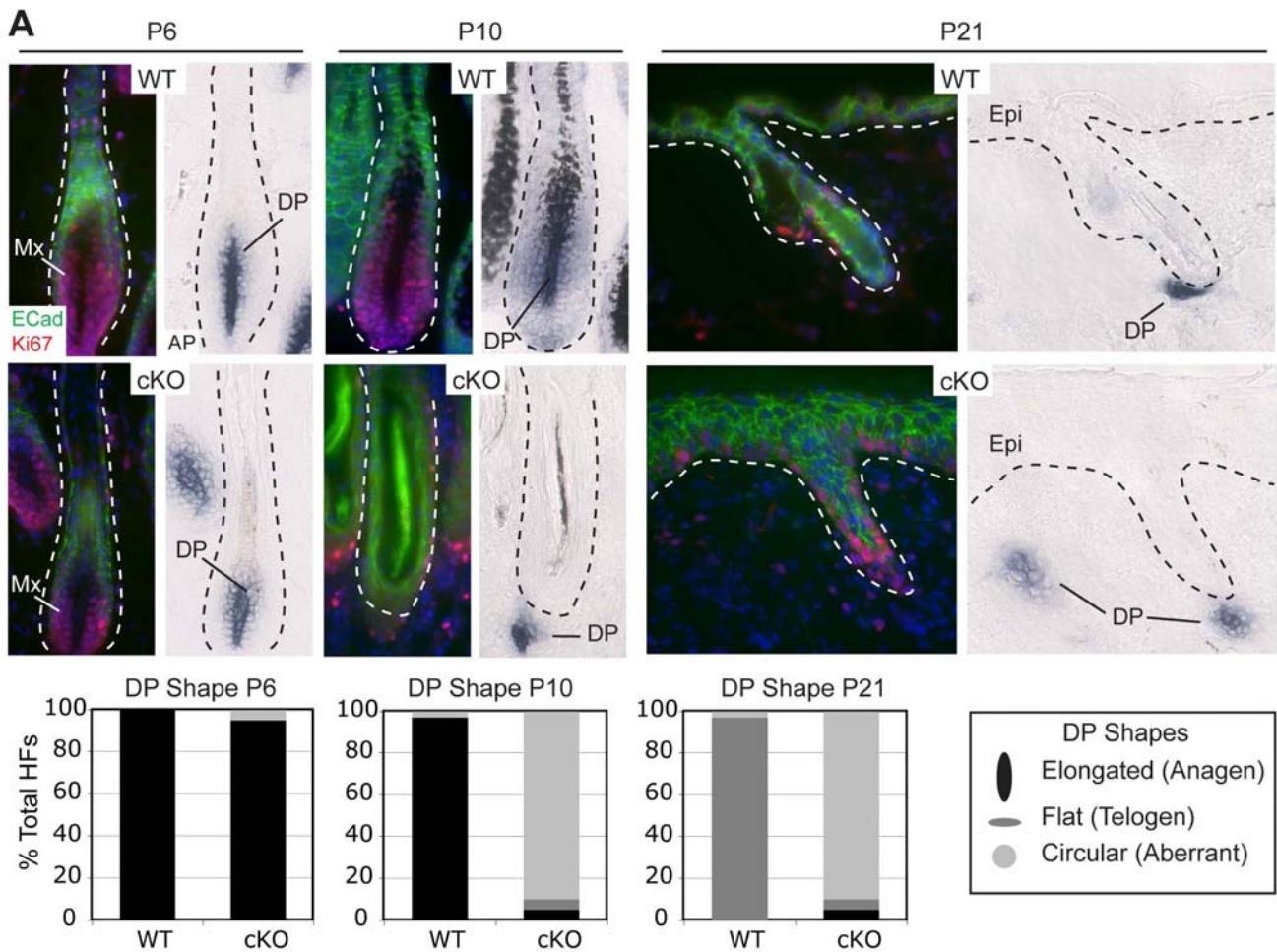


Figure S5. Premature Exit from the Hair Cycle is Concomitant with the Exhaustion of Transit-amplifying Matrix Cells in Sox9 cKO Mice. (A) HF from WT and cKO mice were stained with antibodies against E-Cadherin (ECad) and Ki67 to detect follicle morphology and subsequently stained for alkaline phosphatase (AP) activity to detect dermal papilla cells. Note that the WT DP retains a vertically elongated shape characteristic of anagen between P6 and P10, while the cKO DP switches from an elongated anagen shape at P6 to an abnormally round shape at P10. At P21, WT DPs display a flattened shape characteristic of telogen stage follicles, while cKO DPs are circular, amorphous and frequently found isolated in the dermis without adjacent epithelial cells. Graphs quantify the percentage of DPs with each shape at each time point. Fifty HFs were examined for both WT and cKO at each time point.

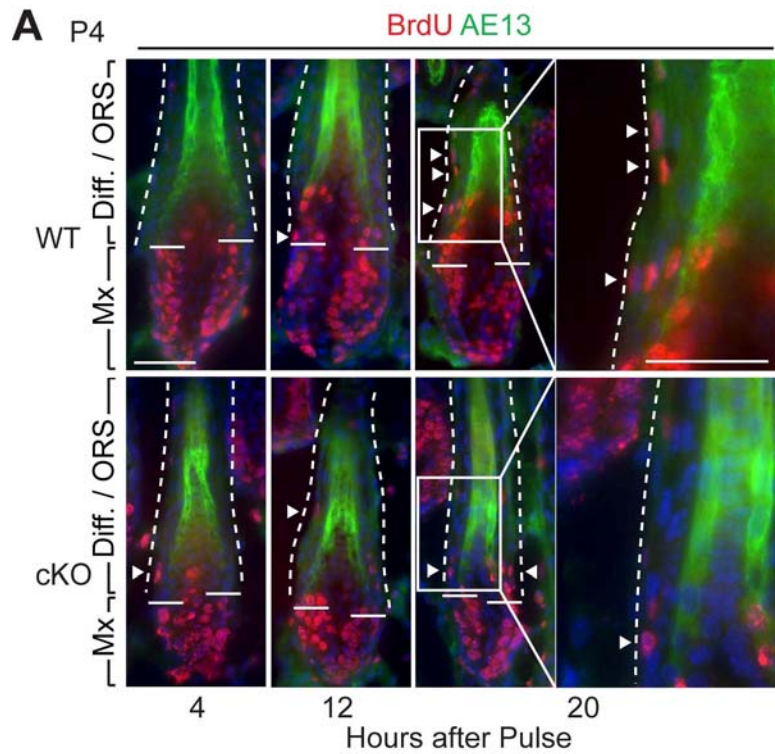


Figure S6. Matrix Proliferation and Differentiation Rates are Relatively Normal in Sox9 cKO Mice, but ORS Input to the Matrix is Impaired. (A) Immunofluorescence microscopy for BrdU and hair keratin (AE13) in representative HF s at indicated time points after a single BrdU pulse at P4. White dotted lines indicate the outside border of the ORS and solid horizontal lines indicate the border between the Mx and the zone of differentiation, demarcated by the lowest AE13 positive cells. Arrowheads indicate examples of BrdU labeled cells in the ORS, which are readily apparent in higher magnification views of HF s at the 20h time point.

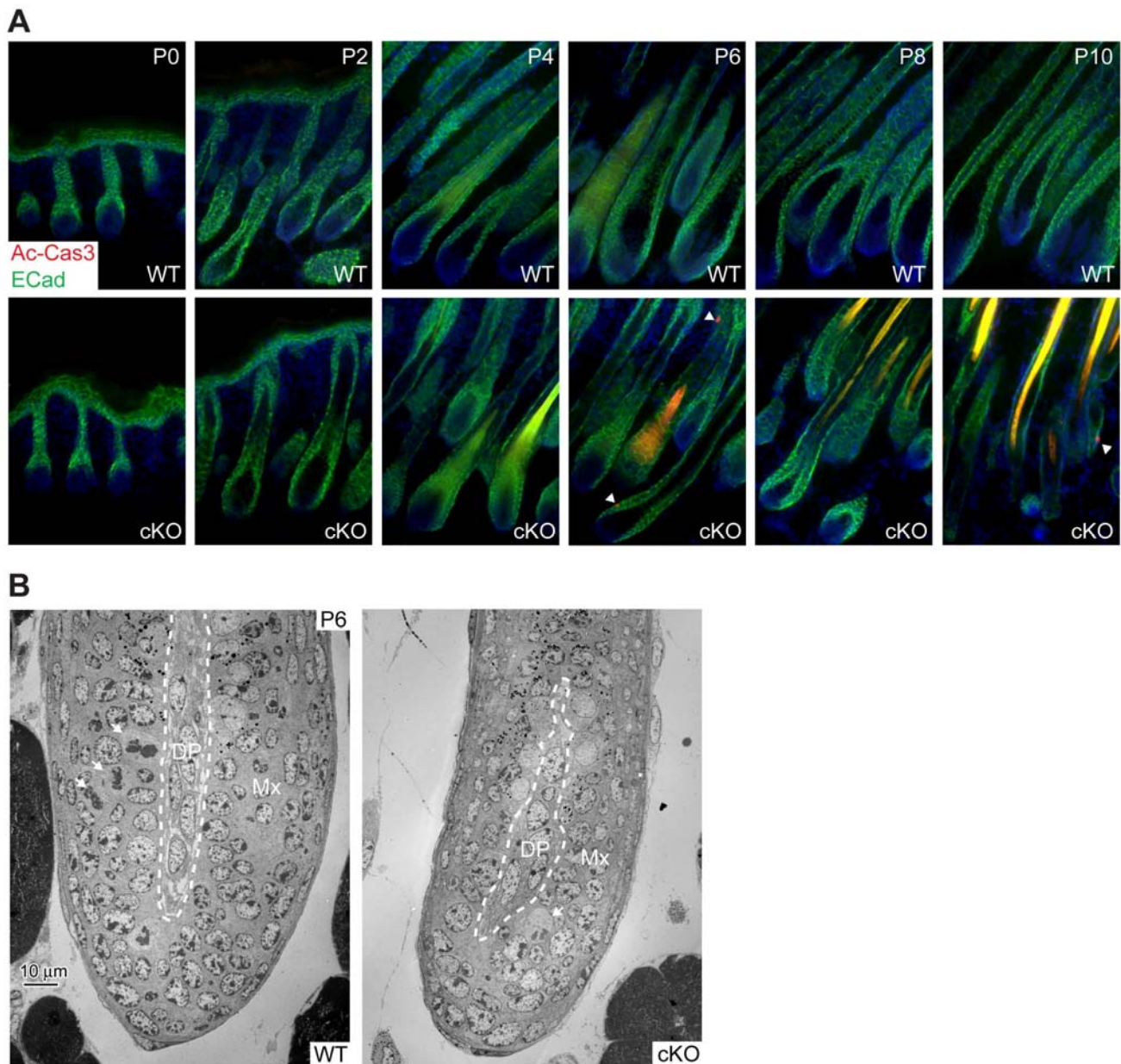


Figure S7. The Reduction in Sox9 cKO Matrix Size is Not Due to Apoptosis. (A) HF from WT and cKO mice at indicated time points were stained with antibodies against activated Caspase-3 (Ac-Cas3), a specific marker of apoptotic cells, and E-Cadherin (ECad). Prior to P6, no apoptotic cells were observed in any compartment of the cKO skin, including the matrix, ORS, interfollicular epidermis and dermis. Beginning at P6 and continuing to P10, rare activated Caspase-3 positive cells could be detected in the skin, but were randomly distributed and not confined to the matrix or ORS. Notably, more than 95% of all cKO follicles remained completely free of activated Caspase-3 staining from P6 to P10. Examples of rare activated Caspase-3 positive cells (arrowheads) are shown in the

cKO at P6 and P10 to illustrate their isolated nature and positive antibody reactivity. **(B)** EM analysis of the matrix from P6 WT and cKO mice reveals the presence of multiple mitotic figures (arrows) and the absence of pyknotic nuclei, indicating a lack of apoptotic cells. DP, dermal papilla; Mx, matrix.

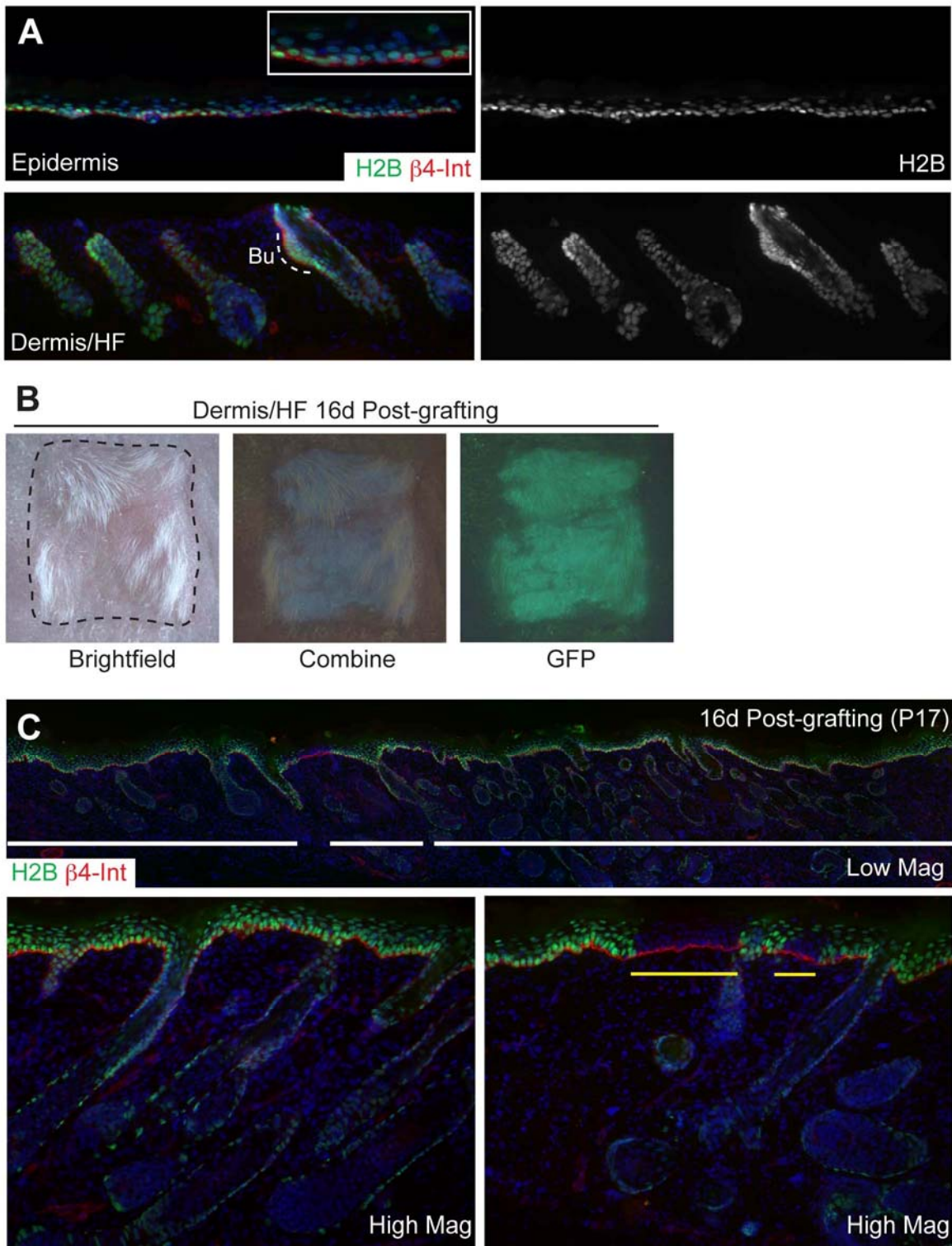


Figure S8. A Split Thickness Grafting Assay can Measure the Contribution of Early HF-derived Cells Towards Repairing the Interfollicular Epidermis. (A) Backskin from P0.5 *K14-H2BGFP* was chemically treated and physically separated into epidermis and dermis/HF components.

Immunofluorescence analysis shows that the epidermis is removed in a single, complete sheet from the underlying dermis, where HFs remain properly oriented. Inset shows β 4-Integrin (β 4-Int), marking the basement membrane, in the isolated epidermis. Note that the bulge region of HFs remains intact and is below the line of separation in the dermis/HF component. **(B)** Brightfield and GFP epifluorescence pictures of a P0.5 *K14-H2BGFP* split thickness graft 16 days after grafting. The presence of hair and GFP expression distinguish the grafted skin from *Nude* epidermis. **(C)** Immunofluorescence analysis of grafted split thickness skin shows robust regeneration of the interfollicular epidermis by H2BGFP positive donor cells. Note that HFs and SGs within the split thickness engrafted skin are morphologically normal, indicating that IFE regeneration has not occurred at the expense of other skin lineages. White horizontal bars mark the extent of H2BGFP positive cell in the IFE at low magnification. High magnification shows one example of a skin region with complete IFE reconstitution and one example of incomplete IFE reconstitution where *K14-H2BGFP* negative *Nude* cells are present in the IFE (region marked by yellow bars). Bu, bulge.

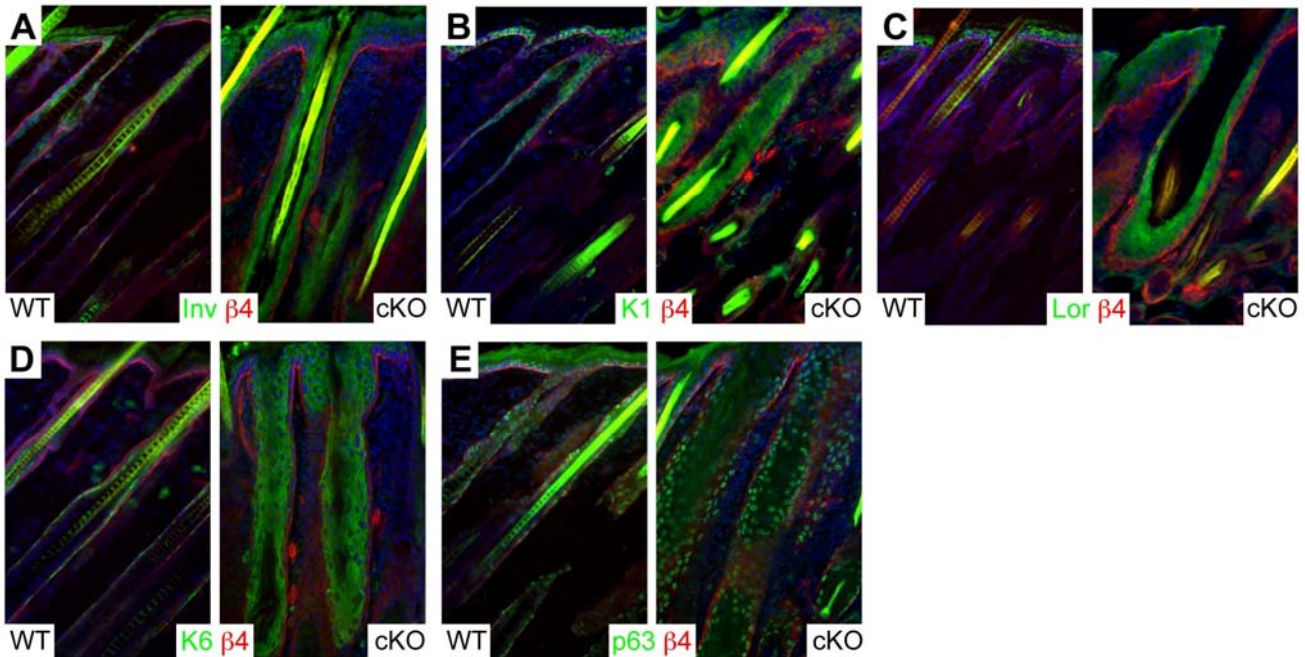


Figure S9. In the Absence of Early SCs, Hair Follicles Adopt Markers of Interfollicular Epidermis. (A,B) Involucrin and keratin 1 mark the spinous layer of the epidermis, and are also normally expressed in a single subbasal layer in the HF. HFs from *Sox9* cKO mice display multiple involucrin and keratin 1 positive cell layers. (C) Loricrin, a marker of the granular layer of the IFE cornified envelope, is not expressed in WT HFs, but is present in multiple layers in cKO HFs. (D) Keratin 6 is normally expressed in the companion layer of the HF and is also induced in suprabasal layers of hyperproliferative IFE. In cKO follicles, multiple layers of keratin 6 positive cells are present in HFs, and extend above the normal location of the companion layer. (E) p63 is normally expressed in a single layer of proliferative basal cells in the IFE and ORS. In cKO HFs, multiple layers of p63 positive cells are present, indicative of a hyperproliferative state. $\beta 4$, $\beta 4$ -Integrin.

Supplemental Reference

Akiyama, H., Lyons, J.P., Mori-Akiyama, Y., Yang, X., Zhang, R., Zhang, Z., Deng, J.M., Taketo, M.M., Nakamura, T., Behringer, R.R., et al. (2004). Interactions between *Sox9* and beta-catenin control chondrocyte differentiation. *Genes Dev.* 18, 1072–1087.